Mature vessel networks in engineered tissue promote graft–host anastomosis and prevent graft thrombosis

Shahar Ben-Shaul[a,b], Shira Landau[a], Uri Merdler[a], and Shulamit Levenberg[a,1]

[a]Department of Biomedical Engineering, Technion-Israel Institute of Technology, 32000 Haifa, Israel; and [b]The Interdepartmental Program for Biotechnology, Technion-Israel Institute of Technology, 32000 Haifa, Israel

Edited by Robert Langer, Massachusetts Institute of Technology, Cambridge, MA, and approved January 3, 2019 (received for review August 23, 2018)

Graft vascularization remains one of the most critical challenges facing tissue-engineering experts in their attempt to create thick transplantable tissues and organs. In vitro prevascularization of engineered tissues has been suggested to promote rapid anastomosis between the graft and host vasculatures; however, thrombotic events have been reported upon graft implantation. Here, we aimed to determine whether in vitro vessel maturation in transplantable grafts can accelerate vascular integration and graft perfusion and prevent thrombotic events in the grafts. To this end, endothelial cells and fibroblasts were cocultured on 3D scaffolds for 1, 7, or 14 d to form vasculature with different maturation degrees. Monitoring graft–host interactions postimplantation demonstrated that the 14-d in vitro-cultured grafts, bearing more mature and complex vessel networks as indicated by elongated and branched vessel structures, had increased graft–host vessel anastomosis; host vessel penetration into the graft increased approximately eightfold, and graft perfusion increased sixfold. The presence of developed vessel networks prevented clot accumulation in the grafts. Conversely, short-term cultured constructs demonstrated poor vascularization and increased thrombus formation. Elevated expression levels of coagulation factors, von Willebrand factor (vWF), and tissue factor (TF), were demonstrated in constructs bearing less mature vasculature. To conclude, these findings demonstrate the importance of establishing mature and complex vessel networks in engineered tissues before implantation to promote anastomosis with the host and accelerate graft perfusion.

tissue engineering | endothelial cells | graft perfusion | vessel maturation

Transplantation of engineered tissue is followed by a narrow time window in which the host vasculature must supply the tissue with blood to avoid ischemia, injury, and necrosis (1–3). Promotion of host vessel invasion into engineered implants has been achieved by delivery of proangiogenic factors (4), careful graft design, and application of various matrix materials or geometries (5–7). In addition, cell combinations (8, 9), such as endothelial cells and mural cells, which together self-assemble into vessel-like structures in the engineered tissues, encourage graft–host vessel anastomosis and graft perfusion (10, 11). While some studies suggest that the presence of endothelial cells in the implanted engineered tissue, regardless of their organization, is sufficient to ensure graft integration and survival (1, 12), others have shown that their assembly into vessel-like structures in the engineered tissue may enhance graft performance postimplantation (6, 8, 10, 13–15). However, it has been shown that engineered vessels may induce thrombosis upon transplantation, leading to reduced graft perfusion and risk of failure (16–19).

Prevascularization of engineered tissues has been induced by prolonged cultivation periods (20), application of mechanical stimuli (14, 21), or culture of endothelial cells (ECs) with various growth factors (22). However, the impact of maturation degree of the engineered vessel network on graft–host vessel anastomosis and graft perfusion upon implantation remains unknown. Vessel maturation is one of the final steps in vasculature development and remodeling and is mediated by adherens junctions and vessel basement membrane rearrangements, as well as the close association between mural cells and the vessel network (23). Abnormal mural cell morphology, lower mural cell counts, and loose attachment of mural cells to vessels result in unstable immature vasculature (24, 25). We hypothesized that the implantation of an engineered construct bearing mature vasculature will improve graft integration.

This study aimed to assess the impact of different degrees of vessel maturation in engineered tissue constructs on graft vascularization and perfusion and on the incidence of blood clot formation upon transplantation.

Results

In Vitro Vessel Network Self-Assembly and Maturation. In vitro spontaneous vessel assembly of GFP-HUVECs (human umbilical vein endothelial cells) and human normal dermal fibroblasts (HNDF) cells embedded in ∼800-μm-thick poly(l-lactic acid)/poly(lactide-coglycolide) (PLLA/PLGA) scaffolds with pore sizes of 212–600 μm was monitored from the day after seeding (Fig. 1 *A*, *i*) and every 3–4 d thereafter for 2 wk. One day after seeding, cells were still solitary; however, by day 4 they were found in clusters throughout the scaffolds (*SI Appendix*, Fig. S1). Sprouting was observed 7 d after seeding and was more extensive on day 10 postseeding; by day 14, flourishing vessel networks were observed throughout the construct, with fourfold more junction points compared with day 1 (Fig. 1*B*). Significantly longer vessels were observed on day 14 compared with vessels of coculture on days 1, 4, 7, and 10 (Fig. 1*B*). To further assess the degree of maturity of the forming vessel network, scaffolds were stained for neuron-glial antigen 2 (NG2), alpha smooth muscle actin (αSMA), and vascular endothelial cadherin (VE-cad) as vasculature markers and for collagen type IV, a component of the

Significance

Rapid graft revascularization, while critical for graft survival, is often not seen in current grafts due to poor basal vascularization. In the present work, we assessed the effect of engineered vessel network assembly and maturation in pre-vascularized constructs prior to implantation on the dynamics of graft integration and perfusion. Grafts bearing highly complex and mature vessel networks were rapidly invaded by host vasculature, which anastomosed with the engineered vessels, promoting their perfusion and reducing blood clot accumulation in the graft. The implantation of grafts with highly mature engineered vessels promises to improve graft integration with the host vasculature and its overall survival.

Author contributions: S.B.-S. and S. Levenberg designed research; S.B.-S. performed research; S.B.-S., S. Landau, and U.M. analyzed data; S.B.-S. and S. Levenberg wrote the paper; and S. Levenberg supervised the research.

The authors declare no conflict of interest.

This article is a PNAS Direct Submission.

Published under the PNAS license.

[1]To whom correspondence should be addressed. Email: shulamit@bm.technion.ac.il.

This article contains supporting information online at www.pnas.org/lookup/suppl/doi:10.1073/pnas.1814238116/-/DCSupplemental.

Published online February 4, 2019.

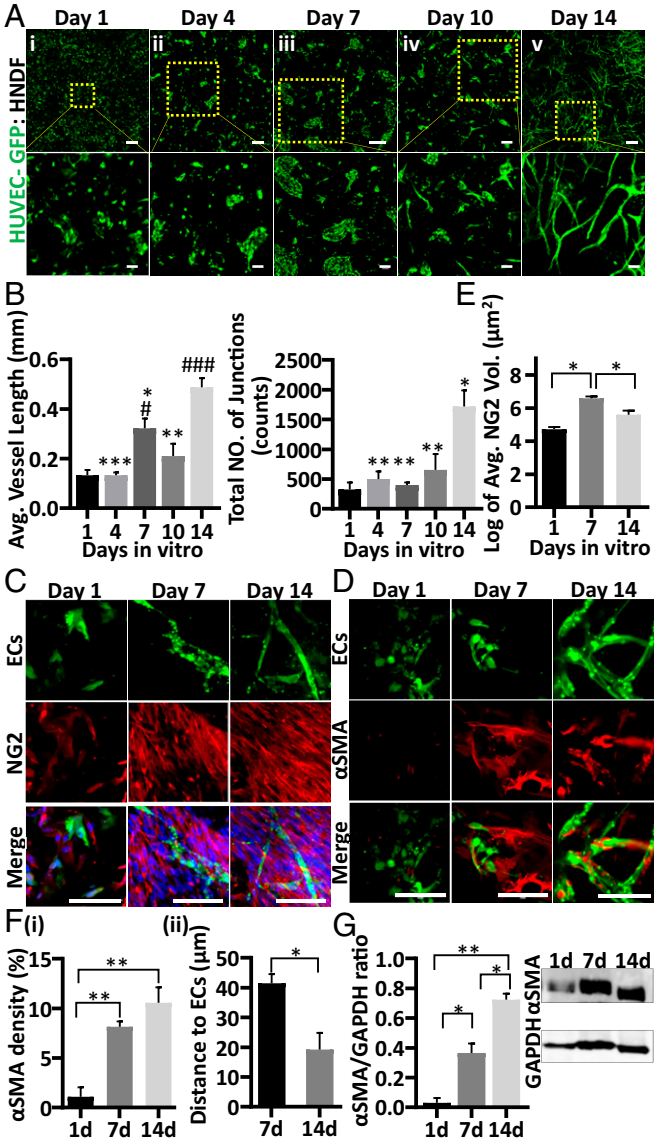

Fig. 1. Dynamics of in vitro vessel-like network formation and maturation. GFP-ECs (green) and HNDFs were embedded in a PLLA/PLGA scaffold and cultured for 14 d. Representative confocal images demonstrating cell morphogenesis and vessel-like network self-assembly in the scaffolds on days 1, 4, 7, 10, and 14 postseeding are shown (*A*, *i–v*, respectively). (Scale bar: 500 μm.) Magnification of the area boxed in yellow (*Lower*). (Scale bar: 100 μm.) Average vessel length and total number of vessel junctions in the scaffolds at the different time points were determined with AngioTool (*B*). Representative confocal images of whole-mount immunofluorescent scaffolds on days 1, 7, and 14, showing vessel-like development, observed via NG2 (red), nuclei (blue) (*C*), and αSMA (red) (*D*). (Scale bar: 100 μm.) Average NG2-positive (*E*) and αSMA-positive (*F*, *i*) cell density on days 1, 7, and 14 of culture, as determined using Imaris software. The distance of αSMA-positive cells from the closest ECs was determined using Imaris distance transformation analysis (*F*, *ii*). Western blot analysis demonstrating αSMA expression in the scaffolds at the three tested time points (*G*). Data are presented as means ± SEM. $n \geq 3$ scaffolds per experiment. * is relative to day 14 and # is relative to day 1 ($^{*}P < 0.05$, $^{**}P < 0.01$, $^{***}P < 0.001$ and $^{\#}P < 0.05$, $^{\#\#}P < 0.01$, $^{\#\#\#}P < 0.001$).

vasculature basement membrane. While NG2-expressing mural cells can be found at early stages of vessel development and during vasculature morphogenesis, αSMA expression is mostly associated with the microvessel network in later stages of maturity (26). NG2 expression was observed 1 d after seeding, increased significantly by day 7, but dropped by day 14 (Fig. 1*E*). In contrast, the number of αSMA-positive cells was negligible 1 d after seeding; it significantly increased by day 7 and rose further by day 14 postseeding (Fig. 1 *F*, *i*). The proximity between αSMA-positive cells and the ECs was significantly greater on day 14 versus day 1 and day 7, with day 14 scaffolds presenting αSMA-expressing cells wrapped around the vessel walls (Fig. 1 *D* and *F*, *i* and *ii*, and *SI Appendix*, Fig. S2). Whole-cell protein analysis confirmed that αSMA expression doubled with each week of culture (Fig. 1*G*). On day 1 of seeding, VE-cad expression was low and scattered in the solitary ECs. However, on day 7, when the ECs formed aggregates, VE-cad expression was serrated and found in ring-shaped structures, and by day 14 of seeding it was observed along the vessel border (*SI Appendix*, Fig. S3). Collagen type IV expression was scattered throughout the scaffolds on days 1 and 7 after seeding. However, by day 14 the engineered vessel networks were surrounded by a continuous collagen type IV basement membrane (*SI Appendix*, Fig. S4).

Engineered-Vessel Network Development upon Implantation. To assess whether in vitro vessel network self-assembly and development alter in vivo vascular organization in the graft, postimplantation vessel length and vascular junction formation dynamics were measured. Scaffolds that were cultured in vitro for 14 d (pre-vascularized constructs) and 1 d (non-pre-vascularized constructs) before implantation were monitored via a dorsal window chamber. Implantation of the non-pre-vascularized constructs was followed by self-organization of the implanted cells into vessel networks, which underwent an increase in both average vessel length and number of network junctions within 7 d of implantation (7.75 and 3 times, respectively). However, a regression in both parameters was observed on days 10 and 14 postimplantation (3.6 and 2.3 times, respectively). Prevascularized scaffolds also displayed a regression in both parameters by day 7 after implantation, but then maintained these values throughout the rest of the assessment period (3.5 and 4.2 times, respectively) (Fig. 2 *A* and *B*). On day 14 postimplantation, both the non-pre-vascularized and prevascularized scaffolds showed mostly similar eccentricity values of the engineered vessel network, with the exception of the most elongated elements (bin 95–100), which were twofold more elongated in prevascularized scaffolds compared with non-pre-vascularized scaffolds (Fig. 2*C* and *SI Appendix*, Fig. S5). Interestingly, comparing 14-d in vitro maturation (prevascularized scaffolds before implantation) to 14-d in vivo development (non-pre-vascularized constructs after 14 d of implantation) revealed more elongated engineered vessels, emphasizing the importance of in vitro culture time before implantation (Fig. 2*C*).

Host Vessel Invasion into Graft. To determine whether prevascularization impacts host vasculature invasion, Alexa-647-anti-CD31 antibodies, which specifically stain the mouse vasculature, were injected into the mouse tail vein; imaging of grafts via the dorsal window chamber followed. Interactions between host and graft vasculature were very minimal during the first week of implantation. On day 7, host vessels began to penetrate the graft margin and advance toward the center of the graft (Fig. 3*A*). To better characterize the progression of host vessel invasion, the graft area was divided into three regions: R1, R2, and R3. On day 10 postimplantation, host vessel coverage in the outer ring of the graft (R1) was significantly higher in scaffolds that had been cultured for 14 d before implantation, with four times more host vessel invasion than in non-pre-vascularized scaffolds. However, by day 14 postimplantation, the same degree of host vessel invasion into R1 was seen in both groups (Fig. 3 *C*, *i*). In the middle ring (R2), no host vessels were observed 10 d after implantation of scaffolds that had been cultured for 1 d before implantation, while prevascularized constructs displayed high host vessel presence in this region. By day 14 postimplantation, host vessels were observed in R2 of both scaffold types but coverage was eightfold higher in the grafts cultured for 14 d compared with the constructs cultured for 1 d before implantation (Fig. 3 *C*, *ii*). In the center of the grafts (R3), no host

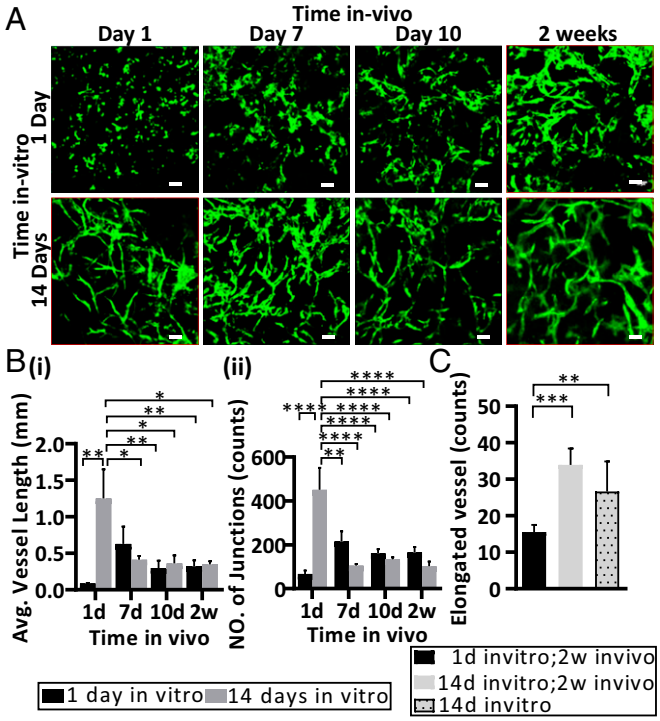

Fig. 2. Vessel-like development in vivo. Representative intravital confocal images of PLLA/PLGA scaffolds seeded with GFP-ECs (GFP) and HNDFs and cultured for 1 d (*Upper*) or 14 d (*Lower*) before implantation in a mouse dorsal window chamber. Images were captured on days 1, 7, 10, and 14 postimplantation (*A*). Average graft vessel length (*B*, *i*) and total number of engineered vessel junctions (*B*, *ii*). Eccentricity analysis of vessels in scaffolds seeded 1 or 14 d before implantation and grafted for 2 wk, or in scaffolds cultured for 14 d in vitro and imaged 1 d postimplantation (red box in *A*); analysis of most elongated vessels (bin 95–100, purple box) in prevascularized and non-pre-vascularized scaffolds 2 wk following implantation versus in scaffolds cultured for 14 d in vitro and not implanted (*C*). Data are presented as means ± SEM. n ≥ 5 (*P < 0.05, **P < 0.01, ***P < 0.001). (Scale bar: 100 μm.)

vessels were observed on day 10 postimplantation in the grafts cultured for 1 d before implantation, while prevascularized grafts exhibited mild host vessel penetration in this region. By day 14 postimplantation, prevascularized grafts contained fourfold more mouse vasculature invasion in R3 compared with the non-pre-vascularized grafts (Fig. 3 *C*, *iii*). Multiple anastomosis sites were observed between the penetrating host vessels and the engineered vasculature. Higher-magnification images of anastomosis events between the grafted ECs and the host vasculature, along with examination of several confocal planes, revealed diverse host-graft vessel interactions: (*i*) engraft wrapping: engineered vessel-like elements wrapped around host vessels in the graft, forming bilayered segments), (*ii*) mosaic vessels: host vessels bridging at least two segments of grafted vessel-like elements, forming patched vessels, and (*iii*) end-to-end connections: tip cells of both host and graft vessels merged to create a single vessel (*SI Appendix*, Fig. S6). The three types of interaction were found to the same degree in both scaffold groups.

Graft Functionality. To examine whether the degree of vessel maturity influenced graft functionality postimplantation, tetramethylrhodamine-isothiocyanate (TRITC)-dextran was injected into the mouse tail vein at various time points following implantation. On day 10 postimplantation, host vessels invading the graft area were functional. Dextran was detected perfusing both the host blood vasculature (*SI Appendix*, Fig. S7) and the engineered vessels (Movie S1). Two weeks after transplantation, ∼30% of the engineered vessels in the prevascularized grafts were perfused (Fig. 4 *A* and *B*, *i*) but only 4–5% of the engineered vessels in grafts cultured for 1 or 7 d before implantation demonstrated blood flow. The average length of the perfused engineered vessels on days 10 and 14 postimplantation was ∼7–10 times greater in the prevascularized grafts (50 and 58 μm, respectively) than in the non-pre-vascularized grafts (5.7 and 8.2 μm, respectively), suggesting that the vessels were sufficiently stable to extend for longer distances (Fig. 4 *B*, *ii*). In addition, a twofold higher accumulation of blood clots was observed in the non-pre-vascularized grafts compared with the prevascularized constructs on days 10 and 14 after implantation (Fig. 5). Protein extracts of scaffolds cultured for 1, 7, or 14 d demonstrated that vWF expression was relatively high on day 1 after seeding while reduced levels were measured on both day 7 and day 14 after seeding (Fig. 6, *i* and *ii*). Similarly, TF expression levels were relatively high on day 1 after seeding and declined over the ensuing 2 wk of in vitro culturing (Fig. 6, *iii*).

Discussion

Graft vascularization plays a fundamental role in the success of tissue and organ transplantations (27, 28); however, the possibility of predicting engineered tissue implantation outcomes based on the graft's vascularization status at implantation has yet to be assessed. Studies have shown that grafting an engineered tissue with ECs alone or after in vitro vessel formation promotes both anastomosis with the host vasculature and graft integration (10, 12, 29, 30).

The formation of in vitro engineered vessels was achieved by coculturing ECs and supporting cells. Dermal fibroblasts were chosen as supporting cells for this study not only due to their proliferative and ECM-secreting abilities but also due to their therapeutic potential and clinical relevance. Their dermal origin allows a minimally invasive isolation procedure, which supports their potential to create autografts and reduces the possibility of graft rejection upon implantation (31–33).

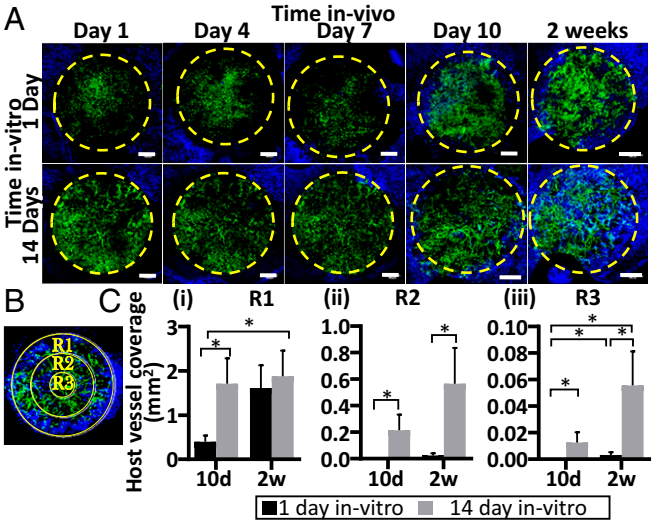

Fig. 3. Host vasculature invasion into the graft. Representative intravital confocal images of host-graft vasculature, as viewed through a dorsal skinfold window on days 1, 4, 7, 10, and 14 postimplantation. Implanted grafts had been cultured for 1 d (*Upper*) or 14 d (*Lower*) before implantation. Graft perimeter (6 mm) is marked by a yellow dashed line, GFP-ECs are in green, and host vessels are in blue (mCD31-AF647 was injected i.v. to visualize host vasculature) (*A*). Three different regions of the graft: R1 represents the outermost ring in the graft perimeter (6 mm), R2 represents the middle ring, and R3 is the center of each graft (*B*). Host vessel coverage (mm^2) analysis in R1, R2, and R3 (*C*, *i–iii*, respectively). Data are presented as means ± SEM. $n \geq 4$ (*P < 0.05). (Scale bar: 1,000 μm.)

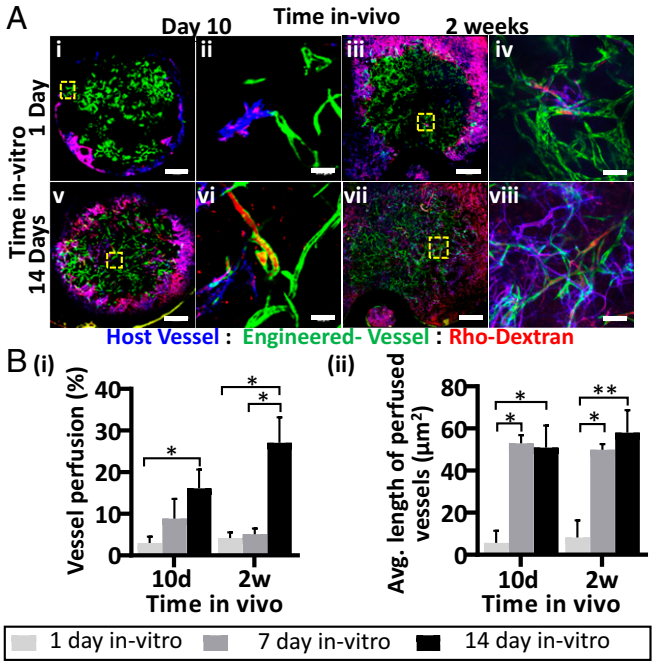

Fig. 4. Host-graft vasculature functionality. Representative intravital confocal images of host-graft vasculature, as viewed through the dorsal skinfold window on days 10 and 14 postimplantation; grafts had been cultured for either 1 d (*Upper*) or 14 d (*Lower*) before implantation. GFP-ECs are shown in green, and host vessels are shown in blue. To visualize blood flow, TRITC-conjugated dextran was injected into the mouse tail vein (red) (*A*). Analysis of the percentage of perfused engineered vessels in the graft cultured for 1, 7, or 14 d in vitro prior to implantation (*B*, *i*) and the average vessel length of the engineered perfused vessels (*B*, *ii*) on days 10 and 14 postimplantation. Data are presented as means ± SEM. $n \geq 3$ (*$P < 0.05$). (Scale bar: 1,000 μm.)

This study showed that the presence of mature and developed vessel networks is essential in promoting host vessel penetration into the graft, graft–host vessel anastomosis, and graft perfusion within 10 d of implantation into a dorsal skinfold chamber in nude mice. It was demonstrated that, upon implantation of non-pre-vascularized grafts, vessel self-assembly occurred in constructs cultured with isolated ECs and supporting cells and was associated with minor host vasculature invasion and anastomosis, mostly in the graft perimeter. In contrast, prevascularized grafts demonstrated enhanced host vessel invasion and integration (Figs. 2 and 3). Although the more developed engineered vessel networks of pre-vascularized grafts underwent a certain degree of regression in both average vessel length and structural complexity upon implantation (Fig. 2*B*), rapid and vast host vessel invasion throughout the graft, with multiple host-graft connections and accompanied by blood perfusion of the grafted engineered vessel networks, was demonstrated. Although the average vessel length at 14 d after implantation was similar in prevascularized and non-pre-vascularized grafts, a significant increase in elongated vessels was observed in the constructs containing the developed vessel networks before implantation (Fig. 2*C*). These features likely promoted graft anastomosis and blood perfusion.

Studies have demonstrated that vessel development can be assessed by the differentiation state of the mural cells surrounding the vessel tubes (23, 34). Vessel network stability and lumen formation can also be demonstrated by the expression and patterning of the endothelial cell-to-cell adherens junctions, marked by VE-cadherin, which play a key role in vascular integrity maintenance (35, 36). It was previously shown that, during cell junction formation, cell-to-cell contacts form serrated rings (i.e., shaped structures), which were associated with early stages of lumen formation in zebrafish embryos (37). These rings were observed on day 7 in our in vitro model. The continuous VE-cad expression along the vessels, which was observed in the day 14 in vitro constructs (*SI Appendix*, Fig. S3), was previously demonstrated in vascular rearrangement processes and shown to be associated with more complex and mature vasculature (38, 39). This expression was also observed on day 14 in our in vitro model (*SI Appendix*, Fig. S3). While NG2-expressing mural cells can be found at early stages of vessel development and during vasculature morphogenesis, αSMA expression is mostly associated with the microvessel network in later stages of maturity (28). The cells at this stage are probably myofibroblasts, although some of them may continue to differentiate to SMCs.

Given the observed αSMA-positive cells wrapped around the vessel network on day 14 of culture and the collagen type IV expression surrounding the engineered vessels (*SI Appendix*, Fig. S4), it can be said that the developed engineered vessel networks formed in vitro were more stable and mature compared with those in scaffolds precultured for 1 or 7 d only. Our previous studies showed that vessel networks developing during 14 d of in vitro culture were not quiescent and still secreted proangiogenic cytokines, which can attract and promote host vessel penetration into the prevascularized graft upon implantation (20, 40). Vessel leakiness was observed in the scaffolds, demonstrated by dextran diffusion from the vessels into the surrounded tissues over time. However, it was very difficult to evaluate the differences in vessel leakiness between the implanted constructs.

Compared with Cheng et al., who described the wrapping and tapping mechanism of host-graft vasculature anastomosis (12), our findings showed three different graft–host vasculature interactions: (*i*) engraft wrapping, as described by Cheng et al., (*ii*) mosaic vessels, with host vessels bridging two grafted vessels, and (*iii*) end-to-end connections between tip cells of both engineered and host vasculature. No preferred connection mechanism was found for either of the tested graft types, and all of the anastomosis configurations led to vessel perfusion (*SI Appendix*, Fig. S6).

The poor engineered vessel perfusion observed in grafts cultured for 1 or 7 d before implantation may have been due to the accumulation of blood clots in the grafts, preventing host vessels from penetrating and anastomosing with the engineered vasculature. Indeed, 10% more clotted area was observed in the non-pre-vascularized grafts in comparison with the prevascularized grafts. Postimplantation graft thrombosis and/or nonfunctional vessels in the prevascularized grafts were reported mostly regarding vessels

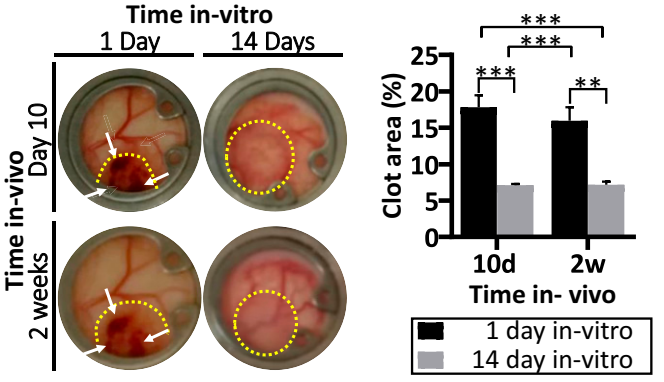

Fig. 5. Non-pre-vascularized constructs show increased clot accumulation upon graft implantation. Representative color images of grafts (marked by a yellow dashed line) as viewed through the dorsal skinfold chamber at 10 and 14 d after implantation. Grafts had been cultured in vitro for 1 or 14 d before implantation. White arrows indicate blood clots in the implanted constructs. Percentage of the grafts containing clots from time of implantation. Data are presented as means ± SEM. $n \geq 5$ (**$P < 0.01$, ***$P < 0.001$).

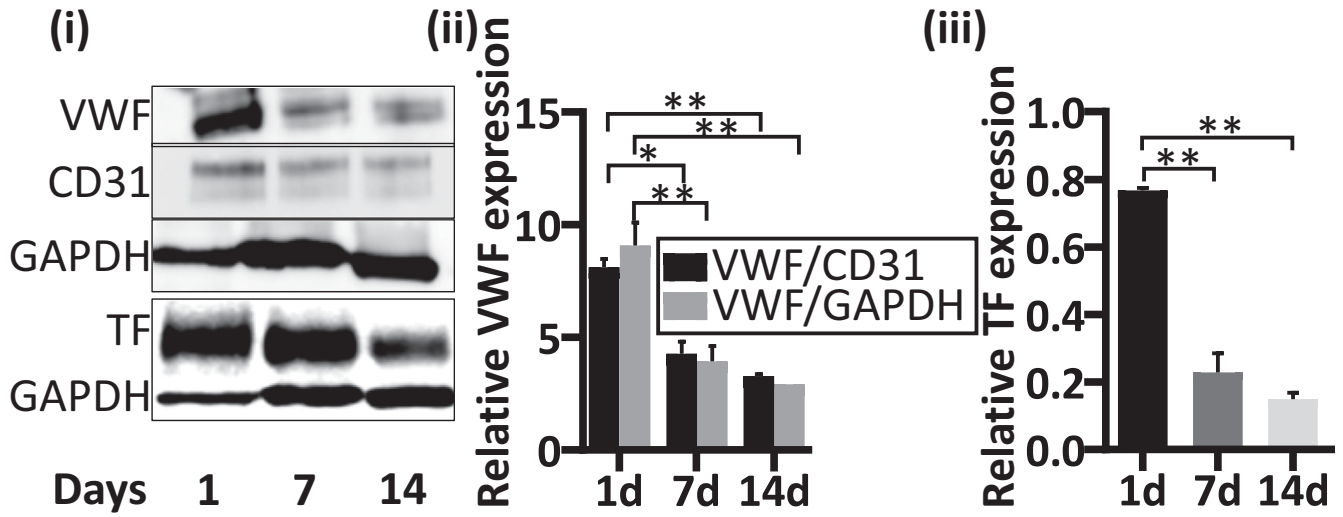

Fig. 6. Expression analysis of coagulation proteins during engineered vessel development in vitro. Whole-cell protein analysis of scaffolds populated with HUVEC-GFP and HNDFs and cultured for 1, 7, or 14 d; each lane represents a pool of proteins extracted from three scaffolds subjected to the same treatment. Immunoblotting was performed with anti-vWF, hCD31, TF, and GAPDH antibodies (*i*). The expression level of vWF was quantified with respect to the endogenous expression levels of both CD31 and GAPDH (*ii*). TF expression level analysis was calculated relative to GAPDH expression (*iii*). Data are presented as means ± SEM. $n \geq 5$ (*$P < 0.05$, **$P < 0.01$).

allowed only 7 or 9 d to form in vitro, as demonstrated in our model (11, 16, 17, 19). In the present analysis, stable and more mature vessels were formed on day 14 of culture (Fig. 1); they may explain why almost no blood clots were detected in the pre-vascularized constructs but a high density of clots was observed in non-pre-vascularized constructs on days 10 and 14 post-implantation. Moreover, clotting was not observed outside the grafts but was found in the graft–host interface and deeper in the graft. Observation of the dextran flow in the engineered microvasculature in the constructs (Fig. 4) indicates the patency of the vasculature. Gebala et al. (41) showed that blood flow is required for formation and expansion of the vessel lumen and for vascular remodeling in a zebrafish model. Lenard et al. (42) showed that initial lumen perfusion in vessel anastomosis is not always stable and may collapse. This highlights the possibility that the immature vessel lumens are also unstable and perhaps even close. White et al. demonstrated that clotting formed in the engineered vessels due to a drop in shear rates below a critical threshold, which may result from the inability of the engineered vessels to conduct blood flow (18). Therefore, we may argue that the immature engineered vasculature shows decreases in lumen patency, diameter, and vessel wall stability, demonstrated by the decrease in αSMA positive cells' wrapping of the engineered vasculature and a low perfusion rate. Changes in blood flow and shear stress may thus contribute to endothelial and platelet activation, which may accelerate the initiation of clotting in grafts bearing immature vasculature.

These findings are supported by those reported by Schultheiss et al., who showed that reseeding decellularized tissue with endothelial progenitor cells led to repopulation of the tissue's capillary and large-vessel networks and prevented immediate thrombus formation upon implantation. In contrast, acellular tissue was associated with thrombosis within 30 min of implantation (30). To further understand the mechanisms inducing thrombosis in grafts cultured for only 1 d before implantation, we analyzed the in vitro expression of proteins known to be involved in the clotting cascade; we detected high levels of both vWF and TF on day 1 after seeding, which decreased by days 7 and 14 of culture (Fig. 6). We propose that the morphology of both ECs and supporting cells, together with the nonmatured vessel structures they form in grafts cultured for only 1 d before implantation, resemble damaged-vessel conditions. Once vessel damage occurs, the endothelial cell lining of the innermost layer of the blood vessel becomes activated and begins to release vWF, which promotes platelet binding and aggregation to form the platelet hemostatic plug (43, 44). In parallel, activated ECs and subendothelial cells express TF, a procoagulant that binds to circulating coagulation factor (f)VII. The complex triggers the coagulation cascade by activating platelet aggregation and cross-linked fibrin to form a stable clot, which seals the injury site to prevent blood loss (44). Therefore, introduction of grafts containing exposed fibroblasts and ECs not organized as stable and developed vessels triggers injury site signals in the host, resulting in coagulation responses. In contrast, grafts with mature vasculature have low levels of both vWF and TF as well as an intact vessel endothelium, allowing for direct connections with host vessels and blood flow with minimal coagulation activity.

Further evidence on the effect of mature engineered vessels was demonstrated by a decrease in platelet adhesion and aggregation in prevascularized grafts compared with grafts cultured for 1 d prior to implantation (*SI Appendix*, Fig. S8). This suggests that implantation of the non-pre-vascularized grafts triggers platelet activation and leads to initiation of the clotting cascade. Blood clot accumulation in the graft may lead not only to graft failure but also to secondary thrombi in distal tissues, which can have life-threatening implications for the host (41).

The suggested prothrombotic phenotype resulting from platelet activation (*SI Appendix*, Fig. S8) due to impaired engineered vasculature is probably a consequence of a complex mechanism. Mediation and recruitment of immune cells into the graft may increase the expression of adhesion molecules such as vascular cellular adhesion molecule 1 (VCAM-1) and intracellular adhesion molecule 1 (ICAM-1) and accelerate clot formation (45, 46). The engagement of CD40L, which is expressed mainly by activated T cells and platelets, with the CD40 receptor increases platelet-leukocyte-endothelium interactions and promotes endothelium adhesion molecule and chemokine synthesis, thus inducing inflammation (46–48).

Endothelial nitric oxide synthase (eNOS) is a potent vessel-remodeling vasodilator (49, 50) with an antithrombotic effect that promotes platelet adhesion and aggregation inhibition (51). eNOS expression and release may be altered as a result of changes in blood flow and shear stress applied on blood vessel walls. Therefore, insufficient and irregular blood flow in immature engineered vessels

may promote thrombosis. The involvement of ECs in platelet and white blood cell (WBC) activation can be further investigated using the presented vascularized graft model.

Graft cellular density may be considered a contributing factor in establishing graft perfusion. Chen et al. reported that increased fibroblast density in endothelial-fibroblast coculture elevated graft perfusion. Moreover, higher fibroblast density promoted early vessel maturation before graft implantation (11). Here we showed that implantation of a denser engineered graft (cultured for 7 d in vitro and still in the early stages of vessel network formation, as shown in Fig. 1) has no significant differences in graft perfusion following 14 d of implantation compared with non-pre-vascularized scaffolds cultured for 1 d in vitro (*SI Appendix*, Fig. S9). However, a significantly higher perfusion rate was observed in grafts bearing mature vessels (14 d in vitro prevascularized constructs). Therefore, we speculate that the maturity of vessels in engineered tissue plays a major role in graft perfusion, and that increasing cellular density may be part of this process.

To conclude, the presented findings reinforce the advantages of establishing a stable and mature vasculature before implantation. These include promotion of graft–host vasculature anastomosis, adequate blood perfusion of the graft, and minimal thrombotic events.

Materials and Methods

Detailed materials and methods are provided in the *SI Appendix*. Briefly, porous scaffolds were fabricated from PLLA/PLGA (50/50%) as previously described (17). GFP-expressing HUVEC and HNDF were embedded with fibrin gel in scaffolds and cultured for 1, 7, or 14 d. Following in vitro culture, the scaffolds were placed in a dorsal window chamber implanted in athymic nude mice. Engineered vessel development, graft perfusion, and host-graft vessel interaction were monitored during 2 wk of implantation using confocal microscopy. To visualize host vasculature, we systemically injected anti-mouse-CD31 and assessed vessel functionality by detection of rhodamine-dextran in the engineered vessels. At the end point, the grafts were retrieved and fixed for further immunohistological analysis.

ACKNOWLEDGMENTS. We thank Janette Zavin for assistance with staining, Oryan Katovitz for assistance with data quantification, Inbal Michael for assistance with the animal model, and Yehudit Posen for editorial assistance in preparing this manuscript. This work was supported by FP7 European Research Council Grant 281501, ENGVASC, by the I-CORE program of the Israeli Planning and Budgeting Committee, and by Israel Science Foundation Grant 1421/16.

1. Koike N, et al. (2004) Tissue engineering: Creation of long-lasting blood vessels. *Nature* 428:138–139.
2. Griffith CK, et al. (2005) Diffusion limits of an in vitro thick prevascularized tissue. *Tissue Eng* 11:257–266.
3. Auger FA, Gibot L, Lacroix D (2013) The pivotal role of vascularization in tissue engineering. *Annu Rev Biomed Eng* 15:177–200.
4. Chen RR, Silva EA, Yuen WW, Mooney DJ (2007) Spatio-temporal VEGF and PDGF delivery patterns blood vessel formation and maturation. *Pharm Res* 24:258–264.
5. Freeman I, Cohen S (2009) The influence of the sequential delivery of angiogenic factors from affinity-binding alginate scaffolds on vascularization. *Biomaterials* 30: 2122–2131.
6. Baranski JD, et al. (2013) Geometric control of vascular networks to enhance engineered tissue integration and function. *Proc Natl Acad Sci USA* 110:7586–7591.
7. Radisic M, et al. (2006) Biomimetic approach to cardiac tissue engineering: Oxygen carriers and channeled scaffolds. *Tissue Eng* 12:2077–2091.
8. Perry L, Flugelman MY, Levenberg S (2017) Elderly patient-derived endothelial cells for vascularization of engineered muscle. *Mol Ther* 25:935–948.
9. Correia C, et al. (2011) In vitro model of vascularized bone: Synergizing vascular development and osteogenesis. *PLoS One* 6:e28352.
10. Levenberg S, et al. (2005) Engineering vascularized skeletal muscle tissue. *Nat Biotechnol* 23:879–884.
11. Chen X, et al. (2009) Prevascularization of a fibrin-based tissue construct accelerates the formation of functional anastomosis with host vasculature. *Tissue Eng Part A* 15:1363–1371.
12. Cheng G, et al. (2011) Engineered blood vessel networks connect to host vasculature via wrapping-and-tapping anastomosis. *Blood* 118:4740–4749.
13. Rouwkema J, de Boer J, Van Blitterswijk CA (2006) Endothelial cells assemble into a 3-dimensional prevascular network in a bone tissue engineering construct. *Tissue Eng* 12:2685–2693.
14. Rosenfeld D, et al. (2016) Morphogenesis of 3D vascular networks is regulated by tensile forces. *Proc Natl Acad Sci USA* 113:3215–3220.
15. Miller JS, et al. (2012) Rapid casting of patterned vascular networks for perfusable engineered three-dimensional tissues. *Nat Mater* 11:768–774.
16. White SM, et al. (2014) Implanted cell-dense prevascularized tissues develop functional vasculature that supports reoxygenation after thrombosis. *Tissue Eng Part A* 20: 2316–2328.
17. Lesman A, et al. (2011) Engineering vessel-like networks within multicellular fibrin-based constructs. *Biomaterials* 32:7856–7869.
18. White SM, et al. (2012) Longitudinal in vivo imaging to assess blood flow and oxygenation in implantable engineered tissues. *Tissue Eng Part C Methods* 18:697–709.
19. Yazdani SK, Tillman BW, Berry JL, Soker S, Geary RL (2010) The fate of an endothelium layer after preconditioning. *J Vasc Surg* 51:174–183.
20. Koffler J, et al. (2011) Improved vascular organization enhances functional integration of engineered skeletal muscle grafts. *Proc Natl Acad Sci USA* 108:14789–14794, and correction (2012) 109:1353.
21. Zohar B, Blinder Y, Mooney DJ, Levenberg S (2018) Flow-induced vascular network formation and maturation in three-dimensional engineered tissue. *ACS Biomater Sci Eng* 4:1265–1271.
22. Kim JH, et al. (2011) The enhancement of mature vessel formation and cardiac function in infarcted hearts using dual growth factor delivery with self-assembling peptides. *Biomaterials* 32:6080–6088.
23. Darland DC, D'Amore PA (1999) Blood vessel maturation: Vascular development comes of age. *J Clin Invest* 103:157–158.
24. Jain RK (2003) Molecular regulation of vessel maturation. *Nat Med* 9:685–693.
25. Benjamin LE, Golijanin D, Itin A, Pode D, Keshet E (1999) Selective ablation of immature blood vessels in established human tumors follows vascular endothelial growth factor withdrawal. *J Clin Invest* 103:159–165.
26. Ozerdem U, Grako KA, Dahlin-Huppe K, Monosov E, Stallcup WB (2001) NG2 proteoglycan is expressed exclusively by mural cells during vascular morphogenesis. *Dev Dyn* 222:218–227.
27. Novosel EC, Kleinhans C, Kluger PJ (2011) Vascularization is the key challenge in tissue engineering. *Adv Drug Deliv Rev* 63:300–311.
28. Rouwkema J, Rivron NC, van Blitterswijk CA (2008) Vascularization in tissue engineering. *Trends Biotechnol* 26:434–441.
29. Mirabella T, et al. (2017) 3D-printed vascular networks direct therapeutic angiogenesis in ischaemia. *Nat Biomed Eng* 1:83.
30. Schultheiss D, et al. (2005) Biological vascularized matrix for bladder tissue engineering: Matrix preparation, reseeding technique and short-term implantation in a porcine model. *J Urol* 173:276–280.
31. Vig K, et al. (2017) Advances in skin regeneration using tissue engineering. *Int J Mol Sci* 18:E789.
32. Kumar VA, Brewster LP, Caves JM, Chaikof EL (2011) Tissue engineering of blood vessels: Functional requirements, progress, and future challenges. *Cardiovasc Eng Technol* 2:137–148.
33. Karlsson LK, Junker JPE, Grenegård M, Kratz G (2009) Human dermal fibroblasts: A potential cell source for endothelialization of vascular grafts. *Ann Vasc Surg* 23:663–674.
34. Gerhardt H, Betsholtz C (2003) Endothelial-pericyte interactions in angiogenesis. *Cell Tissue Res* 314:15–23.
35. Giannotta M, Trani M, Dejana E (2013) VE-cadherin and endothelial adherens junctions: Active guardians of vascular integrity. *Dev Cell* 26:441–454.
36. Dejana E (2004) Endothelial cell-cell junctions: Happy together. *Nat Rev Mol Cell Biol* 5:261–270.
37. Herwig L, et al. (2011) Distinct cellular mechanisms of blood vessel fusion in the zebrafish embryo. *Curr Biol* 21:1942–1948.
38. Bentley K, et al. (2014) The role of differential VE-cadherin dynamics in cell rearrangement during angiogenesis. *Nat Cell Biol* 16:309–321.
39. Franco CA, et al. (2015) Dynamic endothelial cell rearrangements drive developmental vessel regression. *PLoS Biol* 13:e1002125.
40. Landau S, et al. (2017) Tropoelastin coated PLLA-PLGA scaffolds promote vascular network formation. *Biomaterials* 122:72–82.
41. Gebala V, Collins R, Geudens I, Phng L-K, Gerhardt H (2016) Blood flow drives lumen formation by inverse membrane blebbing during angiogenesis in vivo. *Nat Cell Biol* 18:443–450.
42. Lenard A, et al. (2013) In vivo analysis reveals a highly stereotypic morphogenetic pathway of vascular anastomosis. *Dev Cell* 25:492–506.
43. van Hinsbergh VWM (2012) Endothelium–role in regulation of coagulation and inflammation. *Semin Immunopathol* 34:93–106.
44. Yau JW, Teoh H, Verma S (2015) Endothelial cell control of thrombosis. *BMC Cardiovasc Disord* 15:130.
45. van Gils JM, Zwaginga JJ, Hordijk PL (2009) Molecular and functional interactions among monocytes, platelets, and endothelial cells and their relevance for cardiovascular diseases. *J Leukoc Biol* 85:195–204.
46. Lievens D, et al. (2010) Platelet CD40L mediates thrombotic and inflammatory processes in atherosclerosis. *Blood* 116:4317–4327.
47. Freedman JE (2003) CD40-CD40L and platelet function: Beyond hemostasis. *Circ Res* 92:944–946.
48. Phipps RP (2008) CD40: Lord of the endothelial cell. *Blood* 112:3531–3532.
49. Davis ME, Grumbach IM, Fukai T, Cutchins A, Harrison DG (2004) Shear stress regulates endothelial nitric-oxide synthase promoter activity through nuclear factor kappaB binding. *J Biol Chem* 279:163–168.
50. Zhao Y, Vanhoutte PM, Leung SWS (2015) Vascular nitric oxide: Beyond eNOS. *J Pharmacol Sci* 129:83–94.
51. Rudic RD, et al. (1998) Direct evidence for the importance of endothelium-derived nitric oxide in vascular remodeling. *J Clin Invest* 101:731–736.